

First observation of unlocking the locked mode by electrode biasing on J-TEXT tokamak

Zhipeng Chen^{1,*}, Tong Wang¹, Qingquan Yu^{2,*}, Qiming Hu³, Da Li¹, Jie Yang¹, Dongliang Han¹, Chengshuo Shen¹, Minghui Xia¹, Hai Liu⁴, Nengchao Wang¹, Zhuo Huang¹, Zhoujun Yang¹, Zhifeng Cheng¹, Li Gao¹, Yonghua Ding¹, Peng Shi¹, Zhongyong Chen¹, Ge Zhuang⁵, Yunfeng Liang¹ and J-TEXT team[#]

¹ International Joint Research Laboratory of Magnetic Confinement Fusion and Plasma Physics, State Key Laboratory of Advanced Electromagnetic Engineering and Technology, School of Electrical and Electronic Engineering, Huazhong University of Science and Technology, Wuhan, 430074, People's Republic of China

² Max-Planck-Institut für Plasmaphysik, Garching, 85748, Germany

³ Princeton Plasma Physics Laboratory, Princeton NJ 08543-0451, United States of America

⁴ Institute of Fusion Science, Southwest Jiaotong University, Chengdu, 610031, People's Republic of China

⁵ Department of Engineering and Applied Physics School of Physical Sciences, University of Science and Technology of China, Hefei Anhui, 230026, People's Republic of China

E-mail: zpchen@hust.edu.cn, qingquan.yu@ipp.mpg.de

Abstract

Major disruptions, often caused by locked $m/n = 2/1$ modes (m/n is the poloidal/toroidal mode number), are a great threat to a tokamak fusion reactor and should be mitigated or avoided. The locked $2/1$ modes have been unlocked by electrode biasing (EB) for the first time in J-TEXT tokamak experiments. The application of a sufficiently negative EB voltage in plasma edge region quickly changes the phase and amplitude of the locked $2/1$ mode and drives the mode to rotate in about 10-30 milliseconds. For a larger EB current or a smaller locked mode amplitude, the mode is more easily to be unlocked, revealing a new method for mode unlocking and avoiding plasma disruptions.

Keywords: tearing mode, locked mode unlocking, electrode biasing, disruption avoidance

1. Introduction

It is well known that the major disruption is a great threat to the safe operation of a tokamak fusion reactor like ITER^[1-3]. Many disruptions in tokamak plasmas are caused by locked modes (LM)^[4, 5], especially the locked $m/n=2/1$ mode^[6, 7] (m/n is the poloidal/toroidal mode number). The main root cause of disruptions on JET is mode locking^[8, 9]. The error field and the eddy current in conductive wall can generate electromagnetic (EM) torque^[10] to slow down the magnetic island rotation and to lock the tearing mode (TM).

Extensive research efforts have therefore been devoted to the development of massive gas and pellet injection systems for disruption mitigation, in order to protect the device after a major disruption^[11]. Alternatively, it is also important to explore possible methods to stabilize or even suppress the tearing mode to avoid mode locking. One of them is external torque injection, which can drive a flow and flow shear near the rational surface, such as neutral beam injection (NBI)^[12-15]. However, the momentum input from NBI is not expected to be enough in ITER.

Another is local current drive within the magnetic island^[16, 17], such as modulated electron cyclotron current drive (ECCD) to stabilize the neoclassical tearing mode (NTM)^[18, 19] and even unlock the LM with the assistance of rotating resonant magnetic perturbations (RMPs)^[20]. The RMPs are also independently applied to avoid mode locking and unlock the LM^[21-24]. Besides the methods above, electrode biasing, as a traditional auxiliary to improve the confinement through suppressing the turbulence transport at the edge in tokamak^[25-30] and reversed-field pinch plasma^[30-32], has been attempted to mitigate the disruption caused by the MHD activity successfully^[33-36].

In J-TEXT tokamak, an electrode biasing (EB) system has been designed and constructed^[37], which is used to improve confinement and drive local rotation at plasma edge. The previous works show that the application of EB can not only enhance the constraint of edge turbulence by the radial E_r ^[38], but also modulate the tearing mode frequency to stable or unstable state^[39, 40].

Very recently, the unlocking of locked modes has

* Authors to whom any correspondence should be addressed

[#] See the author list of "Y. Liang et al 2019 Overview of the Recent Experimental Research on the J-TEXT Tokamak, Nucl. Fusion 59 112016"

been achieved by electrode biasing (EB) for the first time on J-TEXT tokamak, which has not been reported in the previous work and other devices. In the following experimental results section, the setup of the unlocking experiment is introduced firstly, Then the dynamic unlocking process is displayed and compared to that without biasing. The EB current and LM amplitude function of the unlocking time is also analyzed statistically. In the end, different mechanism relevant to experiment results will be discussed and the conclusion is drawn out.

2. Experimental results

2.1 Experimental setup

The experiments are carried out in Ohmic discharges with a limiter configuration (major radius $R_0 = 105$ cm and minor radius $a = 25.5$ cm)^[41]. The plasma parameters are as the following: plasma current $I_p = 155$ kA, toroidal magnetic field $B_t = 1.65$ T, the safety factor $q_a = 3.3$ at the plasma edge, and the central line-averaged electron density $n_e \sim 1-2 \times 10^{19}$ m⁻³.

In these experiments, the $m/n = 2/1$ TMs are unstable and grow up. They are then locked by resonant magnetic perturbation (RMP) with a dominant 2/1 component calculated in vacuum conditions^[42], to simulate the error field and wall effect. After mode locking, electrode biasing (EB) is applied to unlock the locked mode (i.e. mode unlocking).

The EB system is installed at a midplane port on the low field side^[37]. Using a reciprocating driver, a disc shaped (1.3 cm in thickness and 4 cm in diameter) graphite electrode, mounted on a shaft housed in an insulating sleeve made of boron nitride, is inserted into the plasma with 3 cm($r=22.5$ cm) deeper than the radial position of limiters. The bias voltage U_{EB} in the range of ± 800 V is employed between the electrode and the limiters, and drives a current following the path: power supply, electrode, plasma, limiters, power supply^[29]. The current in the plasma region should flow across the closed flux surfaces between the electrode and limiters and forms a radial current J_r which equals to the current I_{EB} in the electrode. The radial current induces an additional $J_r \times B$ torque into the momentum equilibrium in the edge region and change the local plasma rotation to a new balance between the force and damping^[25]. When a new balance is achieved in J-TEXT tokamak, the local rotation velocity is proportional to the EB current^[43].

The rotating $m/n = 2/1$ TMs are monitored by the routine poloidal and toroidal Mirnov arrays. The phase and amplitude of locked mode are measured

by two sets of the locked mode detectors^[44]. In which, each set contains two saddle loops installed at two opposite toroidal locations outside of the vacuum vessel. The $q = 2$ surface is at $r \sim 19$ cm (i.e. $r/a = 0.74$), measured by electron temperature perturbations from electron cyclotron emission (ECE).^[45]

2.2 Unlocking locked mode

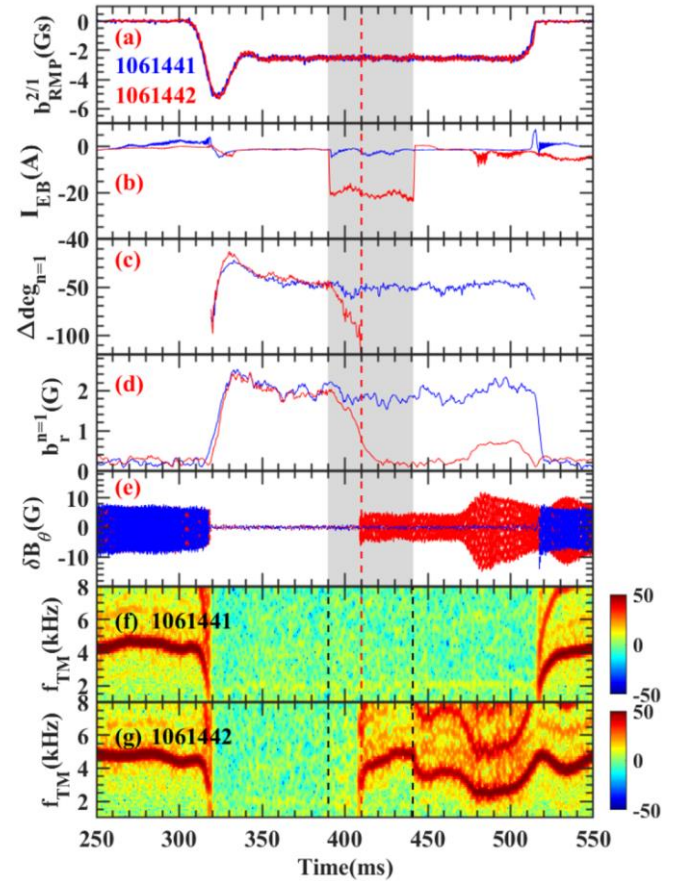


Figure 1. Unlocking of locked mode by EB. Time evolutions of (a) the 2/1 component RMP amplitude, (b) EB current, (c) the phase difference between $n = 1$ locked mode and RMP, (d) locked mode amplitude, (e) high frequency component (>0.5 kHz) of the poloidal magnetic perturbation (δB_θ), (f) and (g) the frequency spectrum from Mirnov probes showing the 2/1 mode frequency for shots 1061441 and 1061442. The shaded region shows the time period of applying EB. The red dashed line shows the time of mode unlocking for shot 1061442.

Figure 1 displays the result of mode unlocking by EB (#1061442, red), compared to a reference discharge without applying EB (#1061441, blue). In both shots, the RMP is turned on at $t = 300$ ms (figure 1(a)), causing the mode locking at $t = 320$ ms. After mode locking, the high frequency component of the magnetic perturbation declines to noise level (figure 1(e)), and the tearing mode frequency decreases from 4.2 kHz to 0 (figure 1(f) and (g)). Meanwhile the locked mode is observed by the locked mode detector (figure 1(c) and (d)). To maintain the locked mode for a sufficiently long time without disruption, the RMP amplitude is ramped down from 6 G to 3.8

G in 20 ms. After that, the phase difference between the locked island and RMP remains unchanged until switching off the RMP, with the $n = 1$ mode amplitude of 1.93 G. In #1061442 an EB current of -20 A is turned on at 390 ms, causing an increase of the phase difference in the counter- I_P direction and a decrease in the mode amplitude. At $t = 409$ ms, the locked mode is unlocked when the phase difference reaches about -95° , in agreement with theoretical prediction^[10]. The mode frequency then quickly increases from 0 to about 3 kHz, followed by a slow increase to about 4.5 kHz. When the EB current is turned off at 440 ms, the mode frequency declines to about 3 kHz. No delay in the change of the locked mode phase is seen from figure 1(c) after the EB current is turned on. Such a fast response of the 2/1 mode to EB current is more evident in experiments without applying RMPs^[39, 40]. An experimental example is shown in figure 2 with $I_P = 150$ kA, $B_t = 1.6$ T, $n_e = 1.3 \times 10^{19}$ m⁻³. The mode frequency is increased immediately following the increase of the EB current, indicating that the EB current in the plasma edge region can quickly affect the rotation of the 2/1 mode located further inside the plasma.

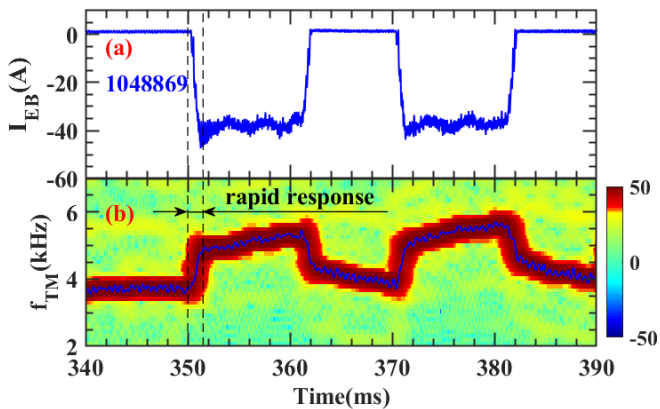


Figure 2. Effect of EB current on rotating tearing mode. Time evolutions of (a) EB current waveform, (b) spectrogram from Mirnov probe data showing the 2/1 mode frequency. The blue curve shows the maximum strength.

2.3 Parameters that affect unlocking process

Figure 3 displays the effect of both EB current and locked mode amplitudes on mode unlocking. The EB current is -20 A at 390ms in #1061442 (blue) and -27A at 390ms in #1061452 (black) during the unlocking, while other plasma parameter and the RMP amplitude are the same. The locked mode is unlocked at about 400ms when the phase difference reaches -100° in #1061452, being earlier than that in #1061442 with a smaller EB current. This suggests that a larger EB current can speed up the unlocking process. A more conclusive results, based on several pulses, is discussed in figure 4b.

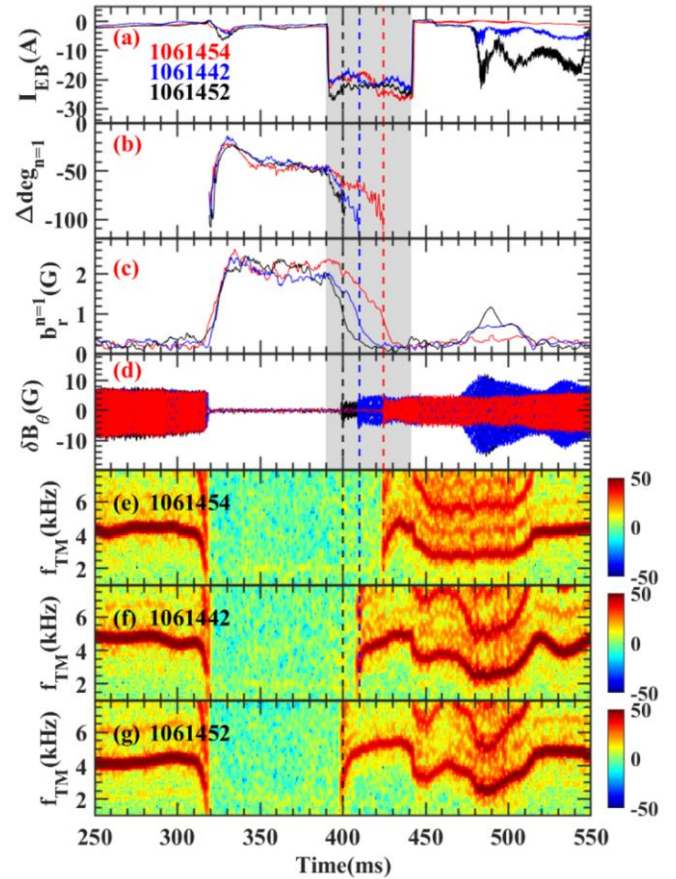


figure 3. Similar to figure 1 but shows the effect of both EB current and locked mode amplitudes on mode unlocking. The black, blue and red dashed lines mark the time of mode unlocking for shots 1061452, 1061442 and 1061454, respectively.

The mode unlocking is also affected by the $n = 1$ locked mode amplitude, as shown in figure 3. The locked mode amplitude before the application of EB is 1.93 G in shot #1061442 (blue) and 2.35 G in #1061454 (red), while other parameters are the same. After an EB current of -20 A at 390ms is turned on in #1061454, the locked mode is unlocked at 424 ms, being later than that in #1061442. This indicates that for the same EB current, more time is required to unlock the locked mode of a larger amplitude.

Figure 4(a) summarizes our statistical experimental results in the plane of the EB current and locked mode amplitude before applying the EB, $b_{r0}^{n=1}$. The triangles (circles) are the cases that the locked modes have (not) been unlocked. The required EB current for mode unlocking increases with locked mode amplitude. The locked mode of a large amplitude cannot be unlocked by a too small EB current. The unlocking time, i.e. the delay between the EB turning-on and mode unlocking times, is shown as a function of the locked mode amplitude in figure 4(b). The cases with about -21 A EB current are shown by triangles. The unlocking time is proportional to the locked mode amplitude. For the cases with an EB current of about -29 A shown in stars, the unlocking time is shorter than that

of -21A EB current.

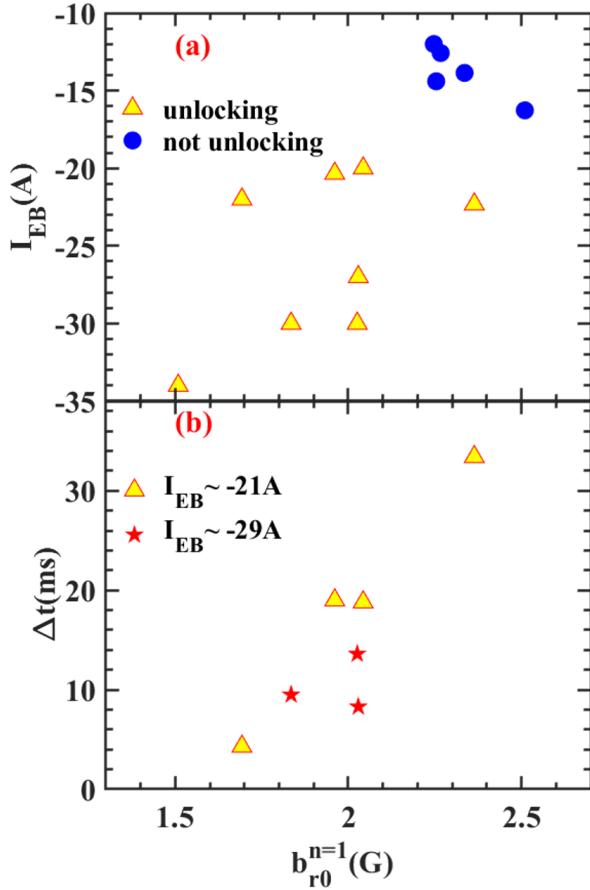


Figure 4. (a) Effect of the EB current and locked mode amplitude on mode unlocking, (b) Effect of locked mode amplitude on unlocking time for $I_{EB} \sim -21$ A/-29 A. $b_{r0}^{n=1}$ is the $b_r^{n=1}$ right before applying EB current, and Δt is the time delay between applying EB current and mode unlocking.

3. Discussion and conclusion

In this reported experiment, the 2/1 magnetic islands are locked by a static helical magnetic perturbation of RMP firstly. Their interaction is well illuminated in the previous research^[10]. The model is based on a cylindrical geometry, intended for interpretate the phenomena in the low beta, large aspect ratio toroidal devices, which is the case of the J-TEXT tokamak. At the simplest phenomenological level of single fluid angular motion equation, the dynamic of magnetic islands is decided by the electromagnetic torque T_{EM} and the fluid viscous torque T_{VS} .

$$L \left(\frac{\partial \Delta \omega}{\partial t} \right) = T_{EM} + T_{VS} \quad (1)$$

Where L is the moment of inertia of plasma inside the magnet island. $\Delta \omega$ represents a deviation of island frequency ω from its natural values ω_0 , the rotation frequency of non-interaction tearing modes. The natural frequency is associated with the typical electron diamagnetic frequency:

$$\omega_0 \sim m \frac{T_e(\text{keV})}{a^2(m) B_t(T)} \quad (2)$$

The poloidal component of electromagnetic torque

T_{EM} produced by RMP coil current could be given by:

$$T_{\theta, EM} \cong -4\pi^2 R_0 \frac{m^2}{\mu_0} |\Psi| |\Psi_{vac}| \sin(-\Delta\phi) \quad (3a)$$

Where Ψ is the perturbed poloidal magnetic flux, and Ψ_{vac} parametrizes the perturbed poloidal flux induced by RMP coil current in the absent of plasma. $\Delta\phi$ is the helical phase shift between the O point of the plasma and the vacuum island, which is corresponding to the phase difference between $n = 1$ locked mode and RMP in the experiment. Assuming the perturbed current to be of helical form as the magnetic island, the toroidal T_{EM} has the relationship with the poloidal component^[10]:

$$T_{\phi, EM} = -\frac{n}{m} T_{\theta, EM} \quad (3b)$$

The fluid viscous torque T_{VS} from outer region to the inner region is given by

$$T_{\theta, VS} = 4\pi R_0 \left[(\mu_{\perp} r^3) \frac{\partial \Delta \Omega_{\theta}}{\partial r} \right]_{r_{s-}}^{r_{s+}} \quad (4a)$$

$$T_{\phi, VS} = 4\pi R_0 \left[(\mu_{\perp} r R_0^2) \frac{\partial \Delta \Omega_{\phi}}{\partial r} \right]_{r_{s-}}^{r_{s+}} \quad (4b)$$

where μ_{\perp} is the coefficient of perpendicular viscosity. $\Delta \Omega_{\theta}$ and $\Delta \Omega_{\phi}$ are the deviation of the island angular velocity from their natural values and $m \Delta \Omega_{\theta} - n \Delta \Omega_{\phi} = \Delta \omega$

r_{s-} and r_{s+} is the location of separatrix of inner and outer region.

When the magnetic island is locked by enough Ψ_{vac} (corresponding to high coil current), $\Delta \omega$ does not vary with time. The equation(1) gives the balance between the electromagnetic torque T_{EM} and the fluid viscous torque T_{VS} . According to equation(3) and (4), the balance in the poloidal direction is

$$\left[(\mu_{\perp} r^3) \frac{\partial \Delta \Omega_{\theta}}{\partial r} \right]_{r_{s-}}^{r_{s+}} = \pi \frac{m^2}{\mu_0} |\Psi| |\Psi_{vac}| \sin(-\Delta\phi) \quad (5)$$

It shows that, the phase shift $|\Delta\phi|$ will increase whilst the Ψ , Ψ_{vac} decreases or the viscous torque is enhanced. The $\Delta\phi \sim 50^\circ$ at 350ms in the figure1(b) and figure 3(b) demonstrates the fluid viscous torque is still strong in this situation. Once the $|\Delta\phi|$ achieves to $\pi/2$, the viscous torque is too strong to be balanced by the electromagnetic torque, then the island is unlocked to rotate. The variation of phase shift during the unlocking is consistent with the $\Delta\phi$ measurement at unlocking moment as shown in figure 1(b) and figure 3(b) within the error of degree measurement. More than that, the Ψ is possible to be weakened during the increase of $\Delta\phi$, which will accelerate the unlocking process, as shown in figure1(c) and figure 3(c).

According to the conclusion above, the EB current is able to interrupt the balance in two ordinary ways. Firstly, the EB current drives the plasma rotation in the edge region between the electrode and the limiter, and further affect the plasma rotation near $q = 2$

rational surface via momentum transport from edge to core^[31, 32, 39]. Under negative biasing current (negative biasing voltage), as that in this experiment, the plasma rotation is accelerated toward the natural rotation direction of TM^[39]. It increases the rotation derivation $\Delta\Omega_\theta$, which strengthens the viscous torque and pulls the locked magnetic island to the unlocking direction. The momentum transport can also increase the flow shear at the rational surface^[34, 39], which is a candidate to weaken the intensity of Ψ , and induces the unlocking.

The other way is that the improved confinement under biasing could increase the electron temperature to heighten the natural frequency according to the equation(2). It could enlarge the rotation derivation $\Delta\Omega_\theta$ toward mode unlocking. The improved confinement can also modify the plasma current to a more favorable profile to stable the TM, which suppressed the MHD activities before their growing up^[35, 46]. However, the plasma temperature and density are enhanced slightly at the beginning of unlocking(390~402ms) as shown in the figure 5(b) and (c) respectively. Then they change obviously when the island is going to rotation(402~408ms), which is more likely caused by a 3-dimension equilibrium distribution in the island. The result shows the confinement is not or hard to be improved once the island is locked, which is reasonably due to the dominant parallel transport along the field line rather than the traverse turbulence transport.

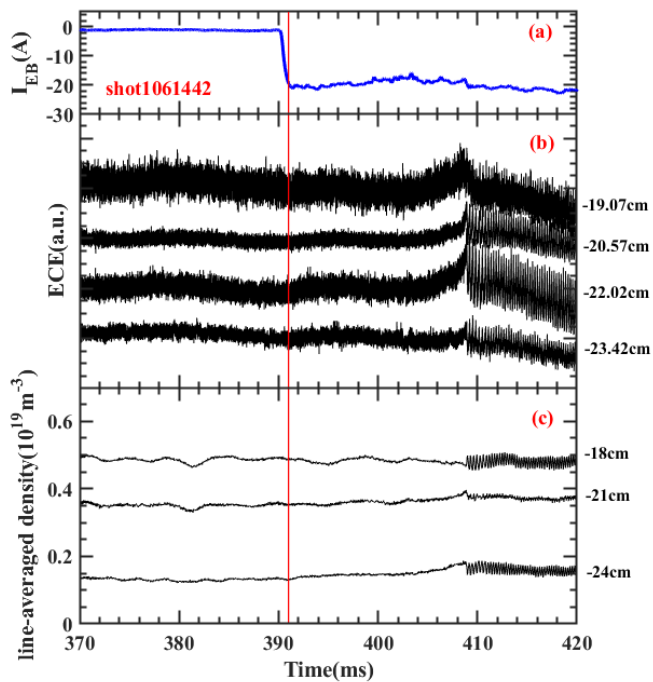


Figure 5. Time evolutions of (a) EB current, (b) ECE signals at the edge, (c) line-averaged density at the edge for shot 1061442. The location marks near the right vertical axis represent the major radiuses relative to R_0 , corresponding to different diagnostic channels.

Though above the scope of the model, reference^[10]

talks about that the modes on different rational surfaces have different natural frequencies and are mismatched. They mutually interact with each other and their interaction can be more sound in a toroidal geometry. Usually the locked 2/1 mode will lead to a locked 3/1 mode due to the toroidal mode coupling, although only the 2/1 mode is identified from the experimental data due to its large amplitude. In our discharges the $q = 3$ surface is in the edge region. If the EB current is sufficiently negative, the local plasma as well as the 3/1 mode is forced to rotate, which will in turn pull the locked 2/1 mode toward mode unlocking via mode coupling. This mechanism is distinctive with those mentioned before, and could be response for the fast response of mode frequency to EB current shown in figure 2 and the experimental results in the previous work^[39, 40].

In general, the interaction between the locked island and RMP can be seen as braking torque in the unlocking process, while the interaction between the locked island and EB as driving torque. For a larger locked mode amplitude, the braking torque is larger, so that the mode unlocking needs more time after applying EB. Increasing the EB current, the driving torque is larger, so that mode unlocking is easier to succeed, and less time is required for mode unlocking. The EB current depends on the local plasma density and temperature, and it can be increased by increasing the electrode size or voltage for given plasma parameters, allowing the flexibility for mode unlocking.

In summary, the application of EB is found to be an effective method to unlock the locked mode for disruption avoidance. The mode unlocking process is affected by the amplitudes of both the EB current and the locked mode. Strong EB current or weak locked island is easy to be unlocked, and vice versa.

Acknowledgements

This work is supported by National Key R&D Program of China (Contract No. 2018YFE0309100), National Magnetic Confinement Fusion Science Program of China (Contract No. 2015GB111001) and the National Natural Science Foundation of China (Contract No. 11905176, 11905078 and 51821005).

References

- [1] F.C. Schuller, Disruptions in tokamaks, Plasma Physics and Controlled Fusion, 37 (1995) A135-A162.
- [2] T.C. Hender, et al., Chapter 3: MHD stability, operational limits and disruptions, Nuclear Fusion, 47 (2007) S128-S202.

- [3] E.J. Strait, et al., Progress in disruption prevention for ITER, *Nuclear Fusion*, 59 (2019) 12.
- [4] M.F.F. Nave, J.A. Wesson, Mode locking in tokamaks, *Nuclear Fusion*, 30 (1990) 2575-2583.
- [5] H. Zohm, et al., Plasma Angular-Momentum Loss by MHD Mode Locking, *Europhysics Letters (EPL)*, 11 (1990) 745-750.
- [6] R.M. Sweeney, et al., Relationship between locked modes and thermal quenches in DIII-D, *Nuclear Fusion*, 58 (2018).
- [7] R. Sweeney, et al., Statistical analysis of $m/n = 2/1$ locked and quasi-stationary modes with rotating precursors at DIII-D, *Nuclear Fusion*, 57 (2017) 016019.
- [8] P.C. de Vries, et al., Statistical analysis of disruptions in JET, *Nuclear Fusion*, 49 (2009) 055011.
- [9] P.C. de Vries, et al., Survey of disruption causes at JET, *Nuclear Fusion*, 51 (2011) 053018.
- [10] R. Fitzpatrick, Interaction of tearing modes with external structures in cylindrical geometry (plasma), *Nuclear Fusion*, 33 (1993) 1049-1084.
- [11] V. Riccardo, J.E. contributors, Disruptions and disruption mitigation, *Plasma Physics and Controlled Fusion*, 45 (2003) A269-A284.
- [12] R.J. La Haye, et al., Islands in the stream: The effect of plasma flow on tearing stability, *Physics of Plasmas*, 17 (2010) 056110.
- [13] R.J. La Haye, et al., Influence of plasma flow shear on tearing in DIII-D hybrids, *Nuclear Fusion*, 51 (2011) 053013.
- [14] R.J. Buttery, et al., The influence of rotation on the β_N threshold for the $2/1$ neoclassical tearing mode in DIII-D, *Physics of Plasmas*, 15 (2008) 056115.
- [15] A. Krämer-Flecken, et al., Heterodyne ECE diagnostic in the mode detection and disruption avoidance at TEXTOR, *Nuclear Fusion*, 43 (2003) 1437-1445.
- [16] C.C. Hegna, J.D. Callen, On the stabilization of neoclassical magnetohydrodynamic tearing modes using localized current drive or heating, *Physics of Plasmas*, 4 (1997) 2940-2946.
- [17] H. Zohm, Stabilization of neoclassical tearing modes by electron cyclotron current drive, *Physics of Plasmas*, 4 (1997) 3433-3435.
- [18] C.C. Petty, et al., Complete suppression of $m/n = 2/1$ neoclassical tearing mode using electron cyclotron current drive in DIII-D, *Nuclear Fusion*, 44 (2004) 243-251.
- [19] R. Prater, et al., Stabilization and prevention of the $2/1$ neoclassical tearing mode for improved performance in DIII-D, *Nuclear Fusion*, 47 (2007) 371-377.
- [20] F.A.G. Volpe, et al., Advanced techniques for neoclassical tearing mode control in DIII-D, *Physics of Plasmas*, 16 (2009) 102502.
- [21] T.C. Hender, et al., Effect of resonant magnetic perturbations on COMPASS-C tokamak discharges, *Nuclear Fusion*, 32 (1992) 2091-2117.
- [22] Q. Hu, Q. Yu, Suppressing magnetic island and accelerating its rotation by modulated resonant magnetic perturbation, *Nuclear Fusion*, 56 (2016) 034001.
- [23] H. Jin, et al., Locked mode unlocking by rotating resonant magnetic perturbations in J-TEXT tokamak, *Plasma Physics and Controlled Fusion*, 57 (2015) 104007.
- [24] Y. Liang, et al., Observations of secondary structures after collapse events occurring at the $q = 2$ magnetic surface in the TEXTOR tokamak, *Nuclear Fusion*, 47 (2007) L21-L25.
- [25] R.J. Taylor, et al., H-mode behavior induced by cross-field currents in a tokamak, *Physical Review Letters*, 63 (1989) 2365-2368.
- [26] I.C. Nascimento, et al., Plasma confinement using biased electrode in the TCABR tokamak, *Nuclear Fusion*, 45 (2005) 796-803.
- [27] H.G. Shen, et al., Observations of zonal flows in electrode biasing experiments on the Joint Texas Experimental tokamak, *Physics of Plasmas*, 23 (2016) 042305.
- [28] G. Van Oost, et al., Turbulent transport reduction by $E \times B$ velocity shear during edge plasma biasing: recent experimental results, *Plasma physics controlled fusion*, 45 (2003) 621.
- [29] R.R. Weynants, et al., Confinement and profile changes induced by the presence of positive or negative radial electric fields in the edge of the TEXTOR tokamak, *Nuclear Fusion*, 32 (1992) 837-853.
- [30] V. Antoni, et al., Electrostatic transport reduction induced by flow shear modification in a reversed field pinch plasma, *Plasma Physics and*

Controlled Fusion, 42 (2000) 83-90.

[31] A.F. Almagri, et al., Momentum transport and flow damping in the reversed-field pinch plasma, *Physics of Plasmas*, 5 (1998) 3982-3985.

[32] D. Craig, et al., Enhanced Confinement with Plasma Biasing in the MST Reversed Field Pinch, *Physical Review Letters*, 79 (1997) 1865-1868.

[33] D. Basu, et al., Disruption avoidance in the SINP-Tokamak by means of electrode-biasing at the plasma edge, *Physics of Plasmas*, 20 (2013) 052502.

[34] P. Dhyani, et al., A novel approach for mitigating disruptions using biased electrode in Aditya tokamak, *Nuclear Fusion*, 54 (2014) 083023.

[35] I.C. Nascimento, et al., Suppression and excitation of MHD activity with an electrically polarized electrode at the TCABR tokamak plasma edge, *Nuclear Fusion*, 47 (2007) 1570-1576.

[36] H.W. Lu, et al., Suppression of MHD activity with limiter biasing in the HT-7 tokamak, *The European Physical Journal D*, 66 (2012) 213.

[37] T.Z. Zhu, et al., The construction of an electrode biasing system for driving plasma rotation in J-TEXT tokamak, *The Review of scientific instruments*, 85 (2014) 053504.

[38] Y. Sun, et al., The influence of electrode biasing on plasma confinement in the J-TEXT tokamak, *Plasma Physics and Controlled Fusion*, 56 (2014) 015001.

[39] H. Liu, et al., Effect of electrode biasing

on $m/n = 2/1$ tearing modes in J-TEXT experiments, *Nuclear Fusion*, 57 (2017) 016003.

[40] T. Wang, et al., The rapid response of $2/1$ tearing mode to electrode biasing in J-TEXT experiments, *Plasma Physics and Controlled Fusion*, 61 (2019) 065017.

[41] Y. Liang, et al., Overview of the recent experimental research on the J-TEXT tokamak, *Nuclear Fusion*, 59 (2019).

[42] B. Rao, et al., Introduction to resonant magnetic perturbation coils of the J-TEXT Tokamak, *Fusion Engineering and Design*, 89 (2014) 378-384.

[43] Y. Sun, et al., Investigations of turbulent transport and intrinsic torque of toroidal momentum at the edge of J-TEXT tokamak with electrode biasing, *Nuclear Fusion*, 56 (2016) 046006.

[44] Y.H. Ding, et al., Analytical compensation of axisymmetric equilibrium fluxes picked up by locked mode detectors in tokamaks, *The Review of scientific instruments*, 85 (2014) 043502.

[45] Z. Yang, et al., Electron cyclotron emission radiometer upgrade on the J-TEXT tokamak, *Review of Scientific Instruments* 87 (2016) 11E112.

[46] D. Basu, et al., Suppression of electric and magnetic fluctuations and improvement of confinement due to current profile modification by biased electrode in Saha Institute of Nuclear Physics tokamak, *Physics of Plasmas*, 19 (2012) 072510.